PHYSICAL REVIEW E **78**, 065301(R) (2008)

# Modeling evaporation of sessile drops with moving contact lines

N. Murisic and L. Kondic
*Department of Mathematical Sciences, Center for Applied Mathematics and Statistics, New Jersey Institute of Technology, Newark, New Jersey 07102, USA*

(Received 23 October 2008; published 31 December 2008)

We consider evaporation of pure liquid drops on a thermally conductive substrate. Two commonly used evaporative models are considered: one that concentrates on the liquid phase in determining the evaporative flux and the other one that centers on the gas-vapor phase. A single governing equation for the evolution of drop thickness, including both models, is developed. We show how the derived governing equation can be used to predict which evaporation model is appropriate for different considered experimental conditions.

DOI: 10.1103/PhysRevE.78.065301 PACS number(s): 47.55.Ca, 47.55.np, 68.03.Fg, 68.15.+e

Evaporating thin films and drops are present in numerous natural situations and applications of technical importance. Coated liquid films, for example, are often left to dry by evaporation. Residual films whose thickness may vary from millimetric in the case of paints to nanometric for photoresist films in semiconductor applications are often desired in a uniform state. However, various kinds of instabilities, many driven by evaporation-related mechanisms, often occur. Evaporative sessile drops are perhaps even more interesting since nonuniform drop thickness and the presence of contact lines (separating liquid, gas, and solid phases) lead to additional effects, such as a possibility of nonuniform evaporation along the liquid-gas interface, temperature gradients, and related Marangoni effects. These effects are crucial in various problems, such as the so-called coffee-stain phenomenon involving the deposition of solid particles dissolved in the liquid close to a contact line [1] and its numerous applications, such as analysis of DNA microarrays [2].

Despite its apparent simplicity, the problem of an evaporating drop on a thermally conducting solid substrate involves a number of physical processes, including mass and energy transfer between the three phases, diffusion, and/or convection of vapor in the gas phase, coupled with complex physics in the vicinity of a contact line. So-called "2-sided" models include processes in both the liquid and gas phases, but lead to a mathematical formulation of significant complexity, even when solid-phase and contact-line issues are not considered [3]. As we discuss below, various simplifications are based on estimating the importance of the relevant physical processes and lead eventually to models which concentrate only on one of the phases (gas or liquid). The estimates, however, involve quantities which are often not precisely known. In this paper, we demonstrate that various assumptions, commonly used in the literature, lead to models which can produce qualitatively different results. The difference in the theoretical results suggests experimental measurements which can be used to decide on which model is appropriate for a particular physical problem. This will allow for a direct comparison between these models including temperature profiles at the evaporating interface.

The complete 2-sided model can be simplified by realizing that thermal conductivity and viscosity of vapor are small compared to the liquid ones. In addition, assuming that the gas phase is convection free, one reduces the 2-sided model to the so-called "1.5-sided" model, which includes the processes in the liquid and the diffusion of vapor in the surrounding gas [4]. An estimate of a typical diffusion time scale, $t_d=l^2/D$, involves the relevant thickness of the gas phase, $l$, and the diffusion constant for, e.g., water vapor $D \approx 10^{-5}$ m$^2$/s. Assuming for a moment that $l$ is on a millimeter scale (comparable to a typical thickness of a drop) leads to $t_d \approx 10^{-2}$ s. The argument that $t_d$ is much shorter than a typical time scale involved in drop evolution has been used to reduce the diffusion equation for vapor concentration $c$ to the Laplace equation [5]. Furthermore, assuming that the evaporation process itself is extremely fast [6] allows one to completely ignore the processes in the liquid for the purpose of finding the mass flux. Therefore, the problem is simplified to $\nabla^2 c=0$ in the gas-vapor domain. Concentrating now on the part of the domain close to the contact line, one realizes an analogy to finding an electric field (mass flux $J$) in the vicinity of a "lens"-shaped conductor (the drop), where $c$ plays the role of electrostatic potential [1]. Typically this lens model assumes a pinned (stationary) contact line. It is unclear *a priori* how crucial this assumption is, since the contact line, even if mobile, evolves slowly [7]. An extensive modeling using the lens-type model has been carried out, implementing both finite-element and lubrication-type approaches [5,8]. Various versions of this model have been used to predict evaporative behavior of (nonpinning) alkane [9] and colloidal drops [10,11] and to study the temperature profiles along the liquid-gas interface [12], among others.

Focusing on the liquid phase, one realizes that the evaporation is limited by two physical processes: heat diffusion through the liquid supplying heat to the interface and evaporation itself (convective contribution to heat transfer can be shown not to be important following the arguments as discussed in, e.g., [13]). In a simple model [3], the first two processes can be related via Biot number, $\mathrm{Bi}=Kp_T L d_0/k$, where $K=\alpha/\sqrt{2\pi R_g T_{sat}}$ and $p_T=Lp_{sat}/(R_g T_{sat}^2)$. Here, $p_{sat}$ is the saturation pressure, $R_g$ is the universal gas constant divided by the molar mass, $L$ is the latent heat of vaporization, $d_0$ is the drop thickness, $k$ is the liquid heat conductivity, $T_i$ and $T_{sat}$ are the interface and saturation temperatures, and $\alpha$ is the accommodation coefficient, describing the probability of phase change. The limit $\mathrm{Bi}\to 0$ implies that the temperature of the liquid-gas interface tends to the temperature of the solid, evaporation itself proceeds in a reaction-limited regime, and the interface is in a state of nonequilibrium [3].

 

$\mathrm{Bi}\to\infty$, on the other hand, indicates that the evaporation is much faster than the heat diffusion through the liquid and that evaporation proceeds in the liquid heat diffusion-limited regime, with the interface being in equilibrium.

While most of the quantities entering the definition of Bi are well known, the value of $\alpha$ is questionable. A variety of $\alpha$'s in the range $O(1)-O(10^{-6})$ have been used in the literature, often without much justification. Using $\alpha\approx 10^{-4}$ (a value to be discussed shortly) yields $\mathrm{Bi}\approx 10^{-2}$, suggesting that the evaporation may proceed in the reaction-limited regime (however, see below for further discussion of this issue). Further insight can be reached by considering Bi as the ratio of the relevant time scale involved in the liquid heat diffusion, $t_l$, and the one involved in the evaporative process itself, $t_e$. Using $t_l=d_0^2/\kappa$, where $\kappa$ is the thermal diffusivity of liquid and $d_0=0.5$ mm, one finds $t_l\approx 1$ s and $t_e\approx 10^2$ s. We note that a similar value is obtained by using $t_e=(d_0^2\rho L)/(k\Delta T)$, where $\Delta T$ is the appropriate temperature scale [14]. Since $t_e\gg t_l$, one may consider a model where the relevant limiting mechanism is the evaporative process itself, and not heat conduction in the liquid; in addition, since $t_e\gg t_d$, this estimate suggests that diffusion of vapor in the gas may be ignored. This "nonequilibrium one-sided" (NEOS) model has been extensively used for evaporative thin films (see [15] for a review), but only few works have applied it to the evaporating drop problem [11,14,16,17]. We note that the argument outlined here for use of the NEOS model is based on the assumption of relatively small relevant thickness $l$ governing the diffusion in the gas phase. Larger $l$ would lead to larger $t_d$, and thus it would be unclear which model is more appropriate. It should be noted, however, that if $t_d$ is large, the assumption of steady-state formulation for the gas concentration is questionable.

The mathematical model implemented here consists essentially of the Navier-Stokes equations coupled with the energy equations for the liquid and solid, and appropriately chosen $J$, in the spirit of the models reviewed in [15]. The boundary conditions are as follows: (i) Fixed temperature at the bottom of the solid substrate; (ii) no slip, no penetration, and continuity of temperature and heat flux across the liquid-solid interface; and (iii) mass balance, energy balance, and normal and shear stress balance at the liquid-gas interface. For the case of spontaneously evaporating drops which we consider, thermocapillary (Marangoni) effects are expected to be significant [18]. These effects are modeled using a simple linear dependence of surface tension on liquid temperature: $\sigma(T)=\sigma_0-\gamma(T-T_0)$, where $\sigma_0$ is the surface tension at room temperature, $T_0=298$ K, and $\gamma=-d\sigma/dT$ ($\gamma>0$ for most liquids). The solid-liquid interaction is modeled using the disjoining pressure approach. A large body of works in the literature (see, e.g., [19,20]) has discussed the details of relevant microscopic physics. Here we choose a simple model with both attractive and repulsive terms, which are often assumed to result from van der Waals (vdW) intermolecular forces, leading to a stable equilibrium liquid layer (precursor film).

The equations and the boundary conditions are nondimensionalized using the following scales: $d_0=0.5$ mm (typical drop thickness) is the length scale; $d_0^2/\nu$, $\nu/d_0$, and $\rho\nu^2/d_0^2$, where $\nu$ is kinematic viscosity and $\rho$ is density of the liquid, are viscous scales for time, velocity, and pressure, respectively; the temperature difference $T-T_{sat}$ is scaled against $\Delta T=T_0-T_{sat}$; finally, the scale for mass flux is $k\Delta T/(d_0L)$. We use a lubrication approximation, although for some considered problems, the contact angle is relatively large ($\Theta\approx 40°$). This approach is supported by finite-element simulations that show that even for large contact angles, the lubrication approach leads to reliable results [5]. In cylindrical coordinates and assuming azimuthal symmetry, we obtain the following fourth-order PDE for the film thickness $h(r,t)$:

$$\frac{\partial h}{\partial t}+EJ+S\frac{1}{r}\left[rh^3\left(h_{rrr}+\frac{1}{r}h_{rr}-\frac{1}{r^2}h_r\right)\right]_r-\frac{E^2}{D}\frac{1}{r}(rJh^3J_r)_r+\frac{\mathrm{Ma}}{\mathrm{Pr}}\frac{1}{r}[rh^2(h+\mathcal{W})J_r]_r+\frac{\mathrm{Ma}}{\mathrm{Pr}}\frac{1}{r}(rJh^2h_r)_r+A\frac{1}{r}\left\{rh^3\left[\left(\frac{b}{h}\right)^3-\left(\frac{b}{h}\right)^2\right]_r\right\}_r+G\frac{1}{r}(rh^3h_r)_r=0. \quad (1)$$

A similar formulation was used in a number of works; see [15] for a review. We used a similar equation to study the instabilities of evaporative isopropyl alcohol (IPA) drops [14]. The main difference between the present case and [14] (in addition to the geometry) is keeping the evaporative flux $J(h)$ explicitly in the formulation, so that Eq. (1) can be used for both considered evaporative models. The terms of Eq. (1) represent the effects due to viscosity, evaporation, capillarity, vapor recoil, Marangoni stresses (two terms), vdW forces, and gravity, respectively. This equation contains the following nondimensional quantities: $E=k\Delta T/(\rho\nu L)$ is the evaporation number; $S=\sigma_0 d_0/(3\rho\nu^2)$, $D=3Y_v/(2\rho)$, where $Y_v$ is the vapor mass content in the gas; $\mathrm{Ma}=\gamma\Delta T d_0/(2\rho\nu\kappa)$ is the thermocapillary Marangoni number; $\mathrm{Pr}=\nu/\kappa$ is the Prandtl number; $\mathcal{W}=kd/(k_s d_0)$, where $d$ is thickness and $k_s$ is the thermal conductivity of the solid substrate, accounts for thermal effects in the solid; $A=\Omega d_0\rho/(3\mu^2 Nb)$ is the nondimensional Hamaker constant, where $\mu$ is viscosity of the liquid; $\Omega=\sigma_0(1-\cos\Theta)$ and $N=(n-m)/[(n-1)(m-1)]$, where we use $(n,m)=(3,2)$; $b=d_{prec}/d_0$, $d_{prec}$ is the precursor film thickness; and $G=-d_0^3\rho^2 g/(3\mu^2)$, where $g$ is gravitational acceleration. Table I lists values of the most important material parameters for IPA and dionized water (DIW).

TABLE I. Table of parameter values for IPA and DIW [21].

| Parameter | IPA | DIW |
|---|---|---|
| $R_g$ (J/kg K) | 138.35 | 461.92 |
| $L$ (J/kg) | $0.79\times 10^6$ | $2.44\times 10^6$ |
| $T_{sat}$ (K) | 256.1 | 286.8 |
| $k$ (W/K m) | $1.35\times 10^{-1}$ | $6.05\times 10^{-1}$ |
| $\rho$ (kg/m$^3$) | 790 | 998 |
| $Y_v$ (kg/m$^3$) | $7.549\times 10^{-3}$ | $1.196\times 10^{-2}$ |
| $\gamma$ (N/K m) | $0.25\times 10^{-3}$ | $0.18\times 10^{-3}$ |
| $\sigma_0$ (N/m) | $2.1\times 10^{-2}$ | $7.2\times 10^{-2}$ |
| $\mu$ (kg/ms) | $2.04\times 10^{-3}$ | $0.9\times 10^{-3}$ |
| $\Theta$ | 6° | 39° |

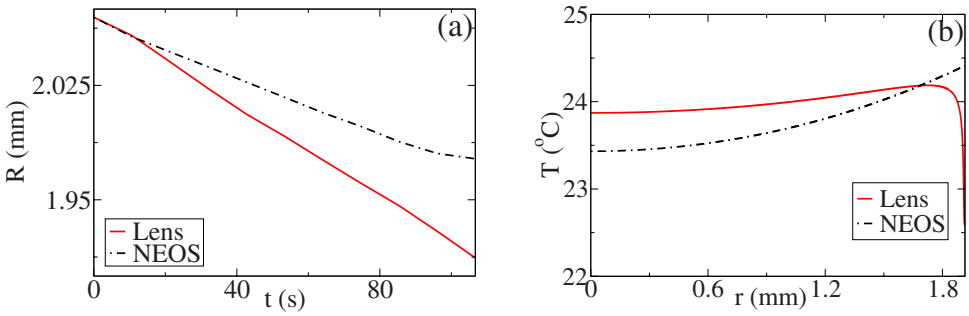


FIG. 1. (Color online) DIW drop: (a) radius $R(t)$ predicted by the two models; (b) temperature of the liquid-gas interface at the end of the time interval shown in (a).

Next, we concentrate on the key point: the evaporative flux $J$. The functional form of $J$ was discussed in more detail elsewhere [22,23]; here, we provide a brief overview. For the lens model, an analogy to the equivalent electrostatics problem yields the following expression for $J(h)$:

$$J(h) = \frac{\chi}{h^{\lambda}}, \tag{2}$$

where the exponent $\lambda$ can be approximated by $\lambda = 0.5 - \Theta/\pi$ [5]. For the NEOS model, based on the kinetic theory of gases, we obtain

$$J(h) = \frac{1}{h + \mathcal{W} + \mathcal{K}}, \tag{3}$$

where $\mathcal{K} = \mathrm{Bi}^{-1}$ [3,14]. For the case of DIW, $\mathcal{K}$ is typically large, as discussed before, and therefore $J(h)$ only weakly depends on $h$. The volatility parameters $\chi$ and $\alpha$ are estimated based on our preliminary experiments, which we report in detail elsewhere [23,24]. We note that for the present purpose of comparing the main features of the results, precise values of these quantities are not crucial. Direct comparison of model predictions to an experiment would require a more precise approach. We use (i) $\chi \approx 5 \times 10^{-2}$ for DIW and $\chi \approx 5 \times 10^{-3}$ for IPA, consistent with experimentally measured volatility from [9]; $\alpha \approx 3 \times 10^{-4}$ for DIW, consistent with the experimental results for drops exposed to open atmosphere [25,26], and based on the same sources, we estimate $\alpha \approx 10^{-3}$ for IPA.

Another important parameter is the precursor film thickness $b$. Although it is typically sufficient to use $b \ll 1$, here we require that the evolution of radius and volume of an evaporating drop not depend on $b$ in any significant manner and find that for $d_0 b \leqslant 0.625$ $\mu$m this requirement is satisfied. Coincidentally or not, this value is consistent with the equilibrium adsorbed film thickness $d_0 b_e \approx 0.5$ $\mu$m for which evaporation stops due to attracting solid-liquid forces [16].

In this work, we concentrate on Si substrates, which are assumed to be sufficiently smooth, so that no pinning of the contact line occurs, in contrast to other works where pinning is known to take place; see, e.g., [1,5,8]. In addition, we assume that the contact angle $\Theta$ does not vary substantially; this assumption is supported by recent experimental data [17]. The numerical simulation of Eq. (1) is carried out using a second-order accurate implicit scheme which is an extension of the one used in [14] to cylindrical geometry. All simulations use as an initial condition the steady-state solution of Eq. (1) obtained by removing the evaporative terms.

Figure 1 compares the predictions of lens and NEOS models for the case of DIW drops. Figure 1(a) shows the evolution of the drop radius, $R(t)$. While the general trend of the results is the same, the speed of the contact line is much larger for the lens model. An explanation for this difference is provided in Fig. 1(b), which shows that the two models lead to qualitatively different temperature profiles along the liquid-gas interface. The resulting Marangoni flow is oppositely directed for the two models. In particular, for the lens model, this flow is from the center of the drop toward the contact line, and it may therefore enhance mass loss and cause more pronounced receding motion of the contact line, as shown in Fig. 1(a). An increase of the temperature as one moves from the center in the NEOS model is a consequence of the fact that the heat supplied from the solid is larger than the heat lost due to evaporation. The lens model, on the other hand, predicts significantly larger evaporative flux in the contact line region, therefore leading to a sharp decrease of temperature there. The temperature increase as one moves away from the center is consistent with previous results which consider solids of similar thermal properties [12,13] or slightly heated solids [18], obtained using a lens-related model, and similar values of $\Theta$ and liquid thermal conductivity, although under the assumption of a pinned contact line. Preliminary experimental results of slightly heated droplets using IR imaging [18] also show an increase of temperature as one moves from the center, at least within the experimental accuracy. We also note that the temperature profile in Fig. 1(b), corresponding to the NEOS model, agrees well with previous numerical results using a similar approach [17]. Our results for the lens model predict a "stagnation point," where the temperature gradient changes sign. A similar temperature maximum has been proposed as an explanation for stagnation points recorded in recent experiments [27]. We note that a nonmonotonous temperature profile is not required to describe the experimental results in [27]: the presence of a stagnation point, based on completely different physical grounds, was extensively discussed as one of the necessary ingredients for the formation of ringlike deposits occurring during evaporation of colloidal drops [10,28]. Finally, we note that our simulations assuming the lens model for smaller values of $\Theta$ leads to monotonically decreasing temperatures along the liquid-gas interface as one moves away from the drop center, in full agreement with earlier results [12,13].

Next, we apply these two models to a more volatile IPA drop. Figure 2 shows the resulting evolution of the drop radius, $R(t)$ [(a)] and the temperature along the liquid-gas in-

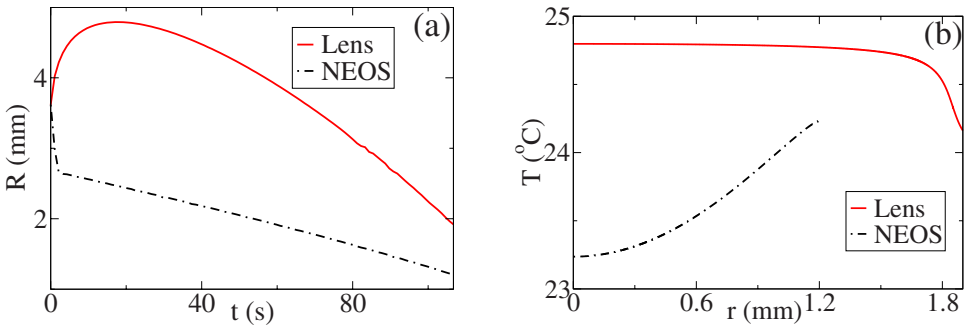


FIG. 2. (Color online) IPA drop: (a) radius $R(t)$ as a result of the two models and (b) temperature profiles of the liquid-gas interface at the final time shown in (a).

terface [(b)]. First, we notice the dramatically different evolution of $R(t)$ for the two models. Considering the temperature profiles in Fig. 2(b) provides immediate understanding of this difference. The Marangoni forces act in opposing directions, leading to a very different evolution. For example, for the lens model, the Marangoni forces act outward, leading to an initial increase of the drop radius [shown in Fig. 2(a)] despite the loss of mass due to evaporation. Preliminary comparison with experiments (discussed in detail in [24]) shows drop evolution which is consistent with the predictions of the lens model [solid line in Fig. 2(a)]. This outcome is perhaps not surprising: increased volatility of IPA compared to the DIW case results in larger vapor production; in addition, the Biot number for IPA is an order of magnitude larger than the one for DIW. The combination of these factors may lead to evaporation which proceeds in the (vapor) diffusion-limited regime. Our hypothesis is further supported by recently confirmed agreement between predictions of the lens model and the experimental data for water-methanol mixtures with volatility characteristics comparable to IPA [29].

In this work we have shown that two commonly used evaporative models may lead to contradictory results for dynamics and in particular temperature profiles of evaporating drops. Future work will discuss in more detail the application of these models to a particular experimental setup. We hope that the results presented here will encourage more elaborate experiments, possibly involving direct measurement of the interfacial liquid-gas temperature, an ultimate test for any evaporation model.

We thank Pierre Colinet, Javier Diez, Yehiel Gotkis, Alex Oron, Bill Ristenpart, and Howard Stone for useful discussions.

[1] R. Deegan *et al.*, Nature (London) **389**, 827 (1997).
[2] R. Blossey, Nature Mater. **2**, 301 (2003).
[3] P. Colinet, J. Legros, and M. Velarde, *Nonlinear Dynamics of Surface-Tension-Driven Instabilities* (Wiley-VCH, Berlin, 2001); B. Haut and P. Colinet, J. Colloid Interface Sci. **285**, 296 (2005).
[4] J. Margerit, M. Dondlinger, and P. Dauby, J. Colloid Interface Sci. **290**, 220 (2005).
[5] H. Hu and R. Larson, J. Phys. Chem. B **106**, 1334 (2002).
[6] Y. O. Popov, Phys. Rev. E **71**, 036313 (2005).
[7] M. Cachile *et al.*, Langmuir **18**, 8070 (2002).
[8] H. Hu and R. Larson, Langmuir **21**, 3963 (2005).
[9] G. Guena, C. Poulard, and A. M. Cazabat, Colloids Surf., A **298**, 2 (2007).
[10] R. Deegan *et al.*, Phys. Rev. E **62**, 756 (2000).
[11] B. Fischer, Langmuir **18**, 60 (2002).
[12] W. Ristenpart, P. G. Kim, C. Domingues, J. Wan, and A. H. Stone, Phys. Rev. Lett. **99**, 234502 (2007).
[13] H. Hu and R. G. Larson, Langmuir **21**, 3972 (2005).
[14] Y. Gotkis, I. Ivanov, N. Murisic, and L. Kondic, Phys. Rev. Lett. **97**, 186101 (2006).
[15] A. Oron, S. H. Davis, and S. G. Bankoff, Rev. Mod. Phys. **69**, 931 (1997).
[16] V. Ajaev, J. Fluid Mech. **528**, 279 (2005).
[17] C. Sodtke, V. Ajaev, and P. Stephan, J. Fluid Mech. **610**, 343 (2008).
[18] F. Girard, M. Antoni, and K. Sefiane, Langmuir **24**, 9207 (2008).
[19] J. N. Israelachvili, *Intermolecular and Surface Forces*, 2nd ed. (Academic Press, New York, 1992).
[20] P. G. de Gennes, Rev. Mod. Phys. **57**, 827 (1985).
[21] *Handbook of Chemistry and Physics*, 78th ed., edited by D. Lide (CRC Press, New York, 1997).
[22] N. Murisic and L. Kondic, Ann. Univ. Ferrara **54**, 277 (2008).
[23] N. Murisic and L. Kondic, e-print arXiv:0802.3207v2.
[24] N. Murisic and L. Kondic (unpublished).
[25] G. T. Barnes, J. Colloid Interface Sci. **65**, 566 (1978).
[26] R. Marek and J. Straub, Int. J. Heat Mass Transfer **44**, 39 (2001).
[27] X. Xu and J. Luo, Appl. Phys. Lett. **91**, 124102 (2007).
[28] G. Berteloot *et al.*, Europhys. Lett. **83**, 14003 (2008).
[29] K. Sefiane, S. David, and M. Shanahan, J. Phys. Chem. B **112**, 11317 (2008).